Biointerface Research in Applied Chemistry
Open-Access Journal (ISSN: 2069-5837)

Article
Volume 13, Issue 5, 2023, 430
https://doi.org/10.33263/BRIAC135.430

Ceramic Membrane-Based on Fly Ash-Clay For River Water Treatment

Selvie Diana [1], Munawar Munawar [1], Saifuddin Saifuddin [1], Nahar Nahar [1], Silmina Silmina [2], Fachrul Razi [2], Nasrul Arahman [2,3,*]

[1] Department of Chemical Engineering, Politeknik Negeri Lhokseumawe, Lhokseumawe 24301, Indonesia; selviediana@pnl.ac.id (S.D.);
[2] Department of Chemical Engineering, Universitas Syiah Kuala, 23111, Banda Aceh, Indonesia
[3] Graduate School of Environmental Management, Universitas Syiah Kuala, Jl.Tgk Chik Pante Kulu No.5, Darussalam, Banda Aceh, 23111, Indonesia
* Correspondence: nasrular@unsyiah.ac.id (N.A.);

Scopus Author ID 25640944900
Received: 2.08.2022; Accepted: 6.10.2022; Published: 16.12.2022

Abstract: Ceramic membrane-based fly ash clay (FAC), sintered at low temperatures, has been implemented in river water treatment. Ceramic membrane with the composition of fly ash: clay 65%: 35% and sintered at 950 for 4 hours has been fabricated. X-ray diffraction (XRD) and energy-dispersive X-ray (EDX) were used to obtain a chemical characterization of fly ash and clay. The filtration process used dead-end and crossflow systems with variations in operating pressure 0.25; 0.50; 0.75, 1.00, and 1.25 bar. The results showed that a ceramic membrane with a crossflow at an operating pressure of 0.75 bar could reflect Pb, Fe, and *Escherichia col*i (*E.coli*) bacteria as much as 96.59%, 95.55%, and 99.29%, respectively. The highest flux amounted to 570.641 L/m^2.h generated at 1.25 bar by the crossflow filtration system. The analysis using scanning electron microscopy (SEM) showed that the pore size of the FAC membrane before the filtration process was 0.9µm, with a membrane porosity of 40.82%. After the crossflow filtration process at 0.75 bar and dead-end filtration at 0.25 bar, the membrane porosity decreased to 39.58 % and 37.97%, respectively. The highest lead intensity is found in the FAC membrane, which is used for crossflow filtration at a pressure of 0.75 bar.

Keywords: clay; fly ash; ceramic membrane; crossflow; dead-end; low temperature.

1. Introduction

Increased pollution from industrial and household waste is causing river water to deteriorate beyond clean water quality standards. Heavy metals and bacteria, such as *E. coli*, are common contaminants in river water with significant toxicity to human health that must be removed in order to meet permitted drinking water and clean water quality standards [1,2]. Ceramic membranes for the microfiltration (MF) process are currently being developed and applied for removing heavy metals and *E. coli* bacteria in water because they have excellent thermal, chemical, and mechanical stability and have high separation efficiency compared to polymer-based membranes [3-5]. Ceramic membranes are generally fabricated of various inorganic materials such as silica, alumina, titania, zirconia, and kaolin, but these materials are relatively expensive. To reduce membrane synthesis costs, low-cost alternative materials are highly recommended [6-8]. Besides, minimizing energy consumption using the sintering method at a low temperature can also be an alternative in the membrane synthesis process to

produce ceramic membranes with lower prices in terms of material and fabrication [9-13]. Cement factories' fly ash, a side waste from the cement and clay industries, is widely found in nature and can be used as a mixture for making ceramic membranes at a relatively low price [14,15]. The particle sizes of around 1.6 μm-2μm of the fly ash and the clay are also very suitable for fabricating ceramic MF membranes [16-19].

Ceramic membranes by mixing fly ash and clay as a primary material using the sintering method at temperatures below 1000° C have been applied, where the membrane with fly ash: clay composition of 60%: 40% and 65%: 35% sintered at 700° C and 1000° C produced a membrane with a pore size of 1.6 μm and 0.64 μm [20,21]. Some researchers have also applied ceramic membranes in river water treatment, such as ceramic membranes made of clay-sawdust-diatomite, sintered at a temperature of 850° C, which can remove turbidity and TDS in river water by 79% and 64% [22]. A membrane with a sintering temperature of 1100 made of clay can also remove up to 97% turbidity using a dead-end flow system [23]. Furthermore, the use of nanofiltration and ultrafiltration ceramic membranes made of montmorillonite, kaolin, tobermorite, magnetite, silica gel, and alumina were reported to be capable of removing heavy metals Cd (II) and Pb (II) up to 97% and 94%, respectively [24,25].

This research will further study river water treatment using ceramic membranes made of fly ash-clay with a composition of 65%–35% sintered at a temperature of 950 °C by modifying the crossflow and dead-end filtration systems and setting variations in operating pressure by 0.25, 0.5, 0.75, 1, and 1.25 bar. This research is expected to produce a relatively inexpensive membrane that can be applied to remove turbidity, TDS, heavy metals like Pb and Fe, and *E. coli* bacteria so that it can achieve water quality standards.

2. Materials and Methods

2.1. Materials.

The primary materials for making membranes are fly ash and clay with particle sizes of 120 μm, with the ratio of fly ash and clay being 65%:35%. The fly ash used in this research came from the local cement industry. Meanwhile, the clay used was purchased from PT. Rudang Jaya in Medan, Indonesia. Sigma Aldrich supplied the polyvinyl alcohol (PVA) used as the adhesive. The river water sample was collected from the Geudong River in Lhokseumawe, Aceh, Indonesia.

2.2. Membrane fabrication.

900 grams of the total fly ash and clay mixed with a composition of 65% fly ash and 35% clay was put into a beaker glass. Furthermore, 36 grams of Polyvinyl Alcohol (PVA) was added. Then as much as 700 ml of water was gradually added to the solution. After that, the mixture was stirred until it formed a paste. The membrane printing was accomplished by pouring the paste into the mold and pressing it. The membrane was removed from the mold and left at room temperature for 7 consecutive days. The membrane was then sintered for 4 hours at 950°C.

2.3. Membrane characterization.

The Archimedes method was used to determine the porosity of the FAC membrane at 950° C sintering temperature as described in Equation 1.

$$\varepsilon(\%) = \frac{W_3 - W_1}{W_3 - W_2} \quad (1)$$

where W_1 is the dry weight of the membrane, W_2 is the dry weight of the membrane calculated inside the water, and W_3 is the fresh weight of the membrane that has been immersed in water for 48 hours.

The pore structure and size of Fly ash, clay, and FAC membranes were analyzed using a Scanning Electron Microscope (SEM) (HITACHI SU3500, Politeknik Manufaktur, Bandung). Fly ash, clay, and FAC membrane elements were analyzed using Energy Dispersive X-Ray (EDX) (EDX OCTANE Pro, Politeknik Manufaktur, Bandung). The fly ash and clay phase's compositions were analyzed using x-ray diffraction (XRD, Analysis Lab, PNL, Indonesia).

Pure water flux (J, L/m^2.hr) ceramic membrane was tested by passing pure water (distilled water) through the membrane module using the dead-end flow and crossflow system with the operating pressure of 0:25, 0.5, 0.75, 1, 1.25 bar. Water flux is calculated based on Equation 2:

$$J = \frac{V_p}{A_m \times t_f} \quad (2)$$

where J is pure water flux (L/m^2.h); Vp is permeate volume (L); Am is effective membrane area (m^2); tf is filtration time (hour)

2.4. River water treatment.

For the ceramic membrane filtration experiment, a water sample as a feed solution was taken from Geudong River, Lhokseumawe District, Aceh Province, Indonesia. Turbidity level, Fe, and Pb concentration in feed and permeate solution were measured using a turbidimeter and atomic absorption spectroscopy (AAS), respectively. Meanwhile, the content of *E. coli* bacteria in the feed and permeate was calculated using the MPN method. The initial river water was pretreated by adding $CaCO_3$ of 20 g/L [26]. Then the river water treatment was carried out through a tubular FAC membrane with an external diameter of 6.5 cm, an internal diameter of 2.5 cm, and a height of 25 cm. The FAC membrane was installed on the module membrane, and river water was flowed by dead-end and crossflow system with pressure variations of 0.25, 0.5, 0.75, 1, and 1.25 bar. The rejection of turbidity, Pb, Fe, and *E. coli* bacteria in the water sample were calculated using Equation 3.

$$R = (1 - \frac{C_p}{C_f}) \times 100 \quad (3)$$

where C_p and C_f are the concentration in the permeate and feed, respectively.

3. Results and Discussion

3.1. Characteristics of fly ash and clay

Fly ash and clay used as ceramic membrane material was characterized in term of crystal structure and chemical composition. Figure 1 shows the results of observations using X-Ray diffraction (XRD), where the crystal structure of fly ash is dominated by SiO_2, $CaSO_4$, TiO_2, and element C, whereas the crystal structure of the clay is composed of $Al_2SiO_5(OH)_4$. The observation of the constituent components of fly ash and clay was also investigated using energy-dispersive X-ray (EDX), as presented in Figure 2 and Table 1. It can be seen that the fly ash and clay are dominated by elements O, Si, and Al.

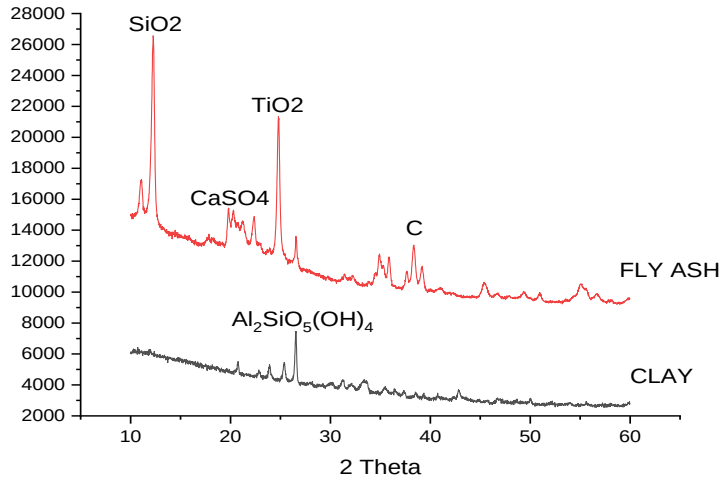

Figure 1. The XRD Pattern of fly ash and clay.

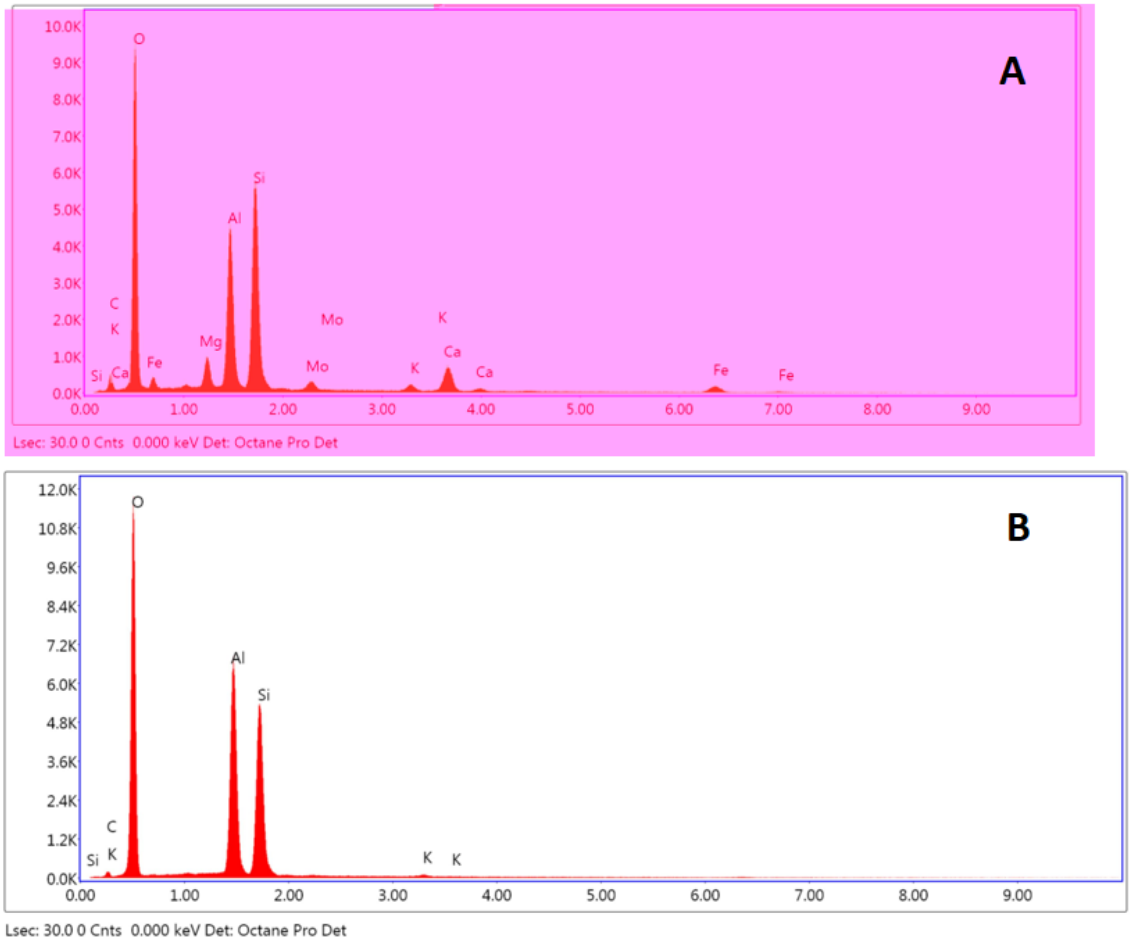

Figure 2. The EDX analysis of **(A)** fly ash and **(B)** clay.

Table 1. Element composition of fly ash and clay.

Element	CK	OK	MgK	AlK	SiK	MoL	KK	CaK	FeK
	Fly ash								
Weightt%	7.38	48.42	2.44	12.36	17.54	1.84	0.94	5.08	3.99
Atomic%	12.13	59.75	1.98	9.04	12.33	0.38	0.47	2.50	1.41
	Clay								
Weightt%	3.57	54.54		20.98	20.48		0.44		
Atomic%	5.69	65.26		14.88	13.96		0.21		

(C: Carbon; K: Potassium; O: Oxygen; Mg: Magnesium; Al: Aluminum; Si: Silica; Mo: Molybdenum; Ca: Calcium; Fe: Iron)

3.2. Characteristics of membrane.

The results of observations using SEM revealed that a ceramic membrane with a composition of fly ash (65%)-clay (35%) has an average pore size of 0.90 µm and porosity of 40.82% (Figure 3). The observations using XRD show that the crystal structure of the FAC membrane is dominated by quartz (SiO_2) illite ($(KH_3O)Al_2Si_3AlO_{10}(OH)_2$) and gypsum ($CaSO_4.2H_2O$) phases (Figure 4).

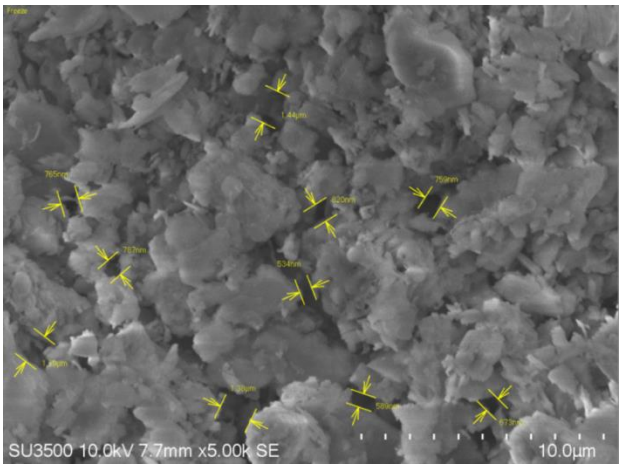

Figure 3. The structure of FAC membrane.

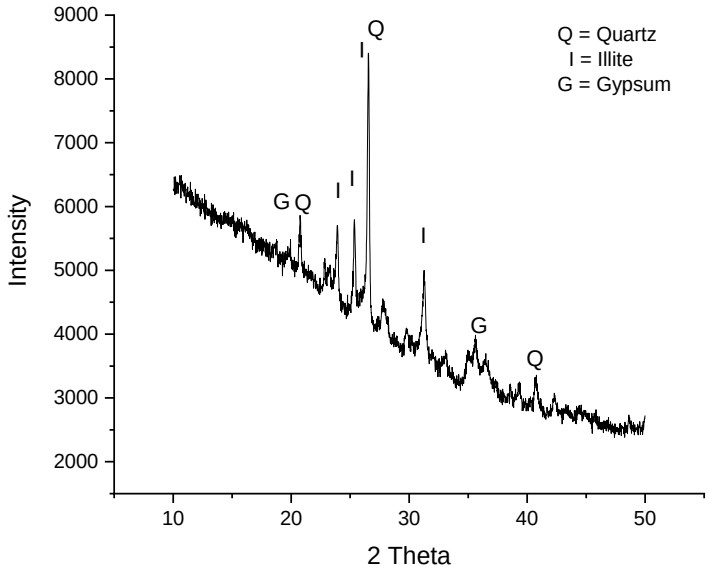

Figure 4. The XRD patterns of FAC Membrane sintered at 950°C.

Figure 5 shows the pure water flux of the membrane obtained at operation pressure from 0.25 to 1.25 bar. The water flux value increases with the increase of filtration pressure. The crossflow filtration system obtains the highest flux of 570.641 L/m2.h at a filtration pressure of 1.25 bar. Pressure as a driving force on the membrane dramatically affects its performance of the membrane, where more molecules in solution will pass through the membrane [27,28]. Based on the characteristics of the FAC membrane, which include the

constituent elements of the membrane, the water flux, and the average pore size, the FAC membrane can be categorized as a microfiltration membrane.

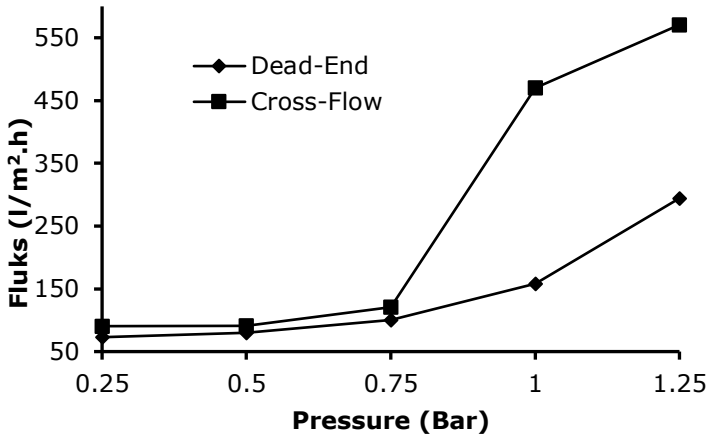

Figure 5. Pure water flux.

3.3. FAC membrane performance for water treatment.

This study applied the FAC ceramic membrane to remove the total dissolved solids (TDS), Pb, Fe, and *E. coli* in the Geudong River, in North Aceh, Indonesia. The filtration flow systems used were dead-end and crossflow. Using the dead-end module, it was known that the highest rejection of the TDS, Pb, Fe, and *E. coli* was generated at a pressure of 0.25 bar, equal to 70.35%, 94.51 %, 91.43% dan 98.67%, respectively (Figure 6). In the case of the crossflow filtration system, the highest rejection of the TDS was generated at a pressure of 0.25 bar, which was 76.35%, while the highest rejection of the other parameter was obtained at an operating pressure of 0.75 bar. The highest rejection of Pb, Fe, and *E. coli* at this condition was 96.59%, 95.55%, and 99.29%, respectively (Figure 6).

At the dead-end flow, the more the rejection of each parameter decreases, the more the pressure increases. The effect of pressure on the dead-end flow system causes compaction in the circuit where the bait flow passes through the membrane and particles accumulate on the membrane surface; as a result, it causes the formation of cake on the membrane to occur more quickly [29-32]. On the other hand, the rejection of each parameter increased to a pressure of 0.75 bar, and rejection decreased at one bar, indicating deformation of the pore size due to an increase in pressure. Only a part of the feed water flows through the membrane pores to produce permeate in the crossflow system. Another part of the feed component flows through the membrane surface so that the colloid and suspended solids retained by the membrane will continue to be carried away into the backflow [33-35]. Thus, the cake formation on the membrane surface with a crossflow system can be avoided because the deposition of particles on the membrane surface will be swept away by the pressure of the feed flow [36].

Table 2. Water quality analysis for the river water and permeate for crossflow filtration at 0.75 bar.

	TDS(mg.L^{-1})	Pb (mg.L^{-1})	Fe (mg.L^{-1})	E.Coli(MPN/100 ml)
Feed Water	344	0.93	2.125	2100
Permeate	95	0.031	0.12	15
WHO Standard	600	0.01	0.3	0
National Standard	1000	0.05	1	0

Table 2 reveals the content of TDS, Fe, and Pb in the permeate has achieved the water quality standards according to WHO drinking water standards [37] and national clean water standards based on Ministerial Regulation No. 32/Menkes/Per/IX/2017 [38] for either dead-end systems or crossflow.

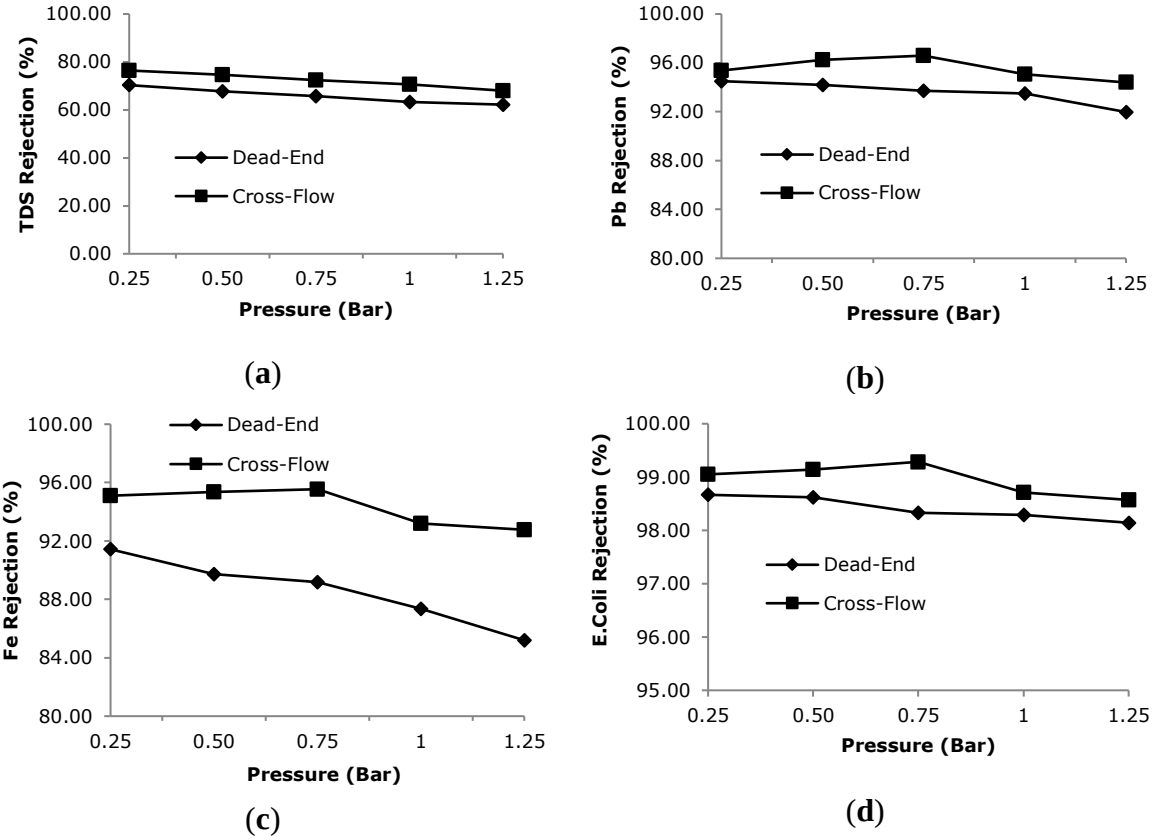

Figure 6. The Rejection of **(a)** TDS, **(b)** Pb**, (c)** Fe**,** and **(d)** *E.coli* bacteria.

Figures 7 show the structure of the FAC membrane after filtration of the river water sample. The structure of the FAC membrane before filtration had a porosity of 40.82% with a pore size of 0.9 µm (Figure 3). The porosity of the FAC membrane after crossflow filtration decreased to 39.58% at 0.75 bar. The porosity of the FAC membrane also decreases during dead-end filtration (37.97% at 0.25 bar).

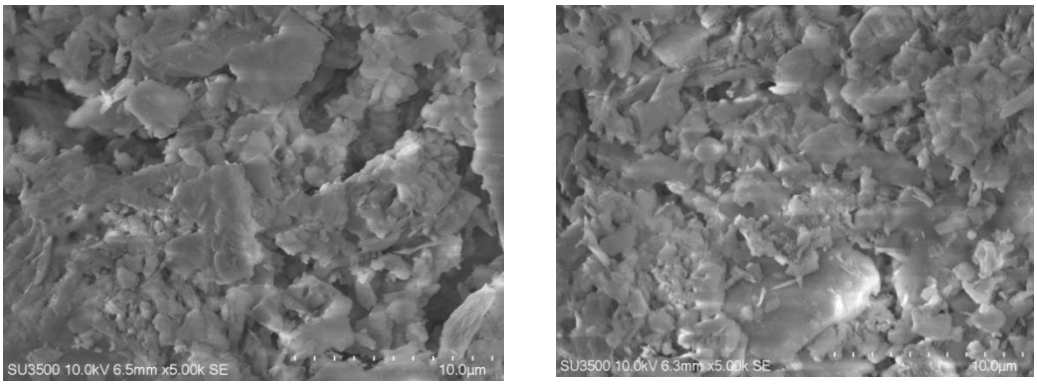

(a) (**b**)

Figure 7. The Structure of FAC Membrane after **(a)** crossflow filtration and **(b)** dead-end filtration**.**

The change in membrane structure is due to polarization phenomena on the membrane surface. The solutes stick to the membrane surface, so the membrane's pore size decreases. These solutes accumulate on the membrane surface and return to the feed stream by back diffusion [39,40]. The solute concentration on the membrane surface was much greater than the solvent concentration in the permeate or the bait. Polarization on the membrane surface may decrease the rejection of turbidity, Pb, Fe, and *E. coli* bacteria as the pressure increases in the dead-end flow system.

Figure 8 shows the crystal structure of each FAC membrane used for dead-end and crossflow filtration processes with pressure variations of 0.25, 0.5, 0.75, 1, and 1.25 bar. The crystal structure of each membrane is dominated by quartz (SiO_2), illite ($Al_2Si_3AlO_{10}(OH)_2$), Magnetite ($FeFe_2O_4$), and Lead (Pb). The highest lead intensity is found in the FAC membrane used for crossflow filtration at a pressure of 0.75 bar, where the percentage of rejection obtained in this filtration process was 96.59%.

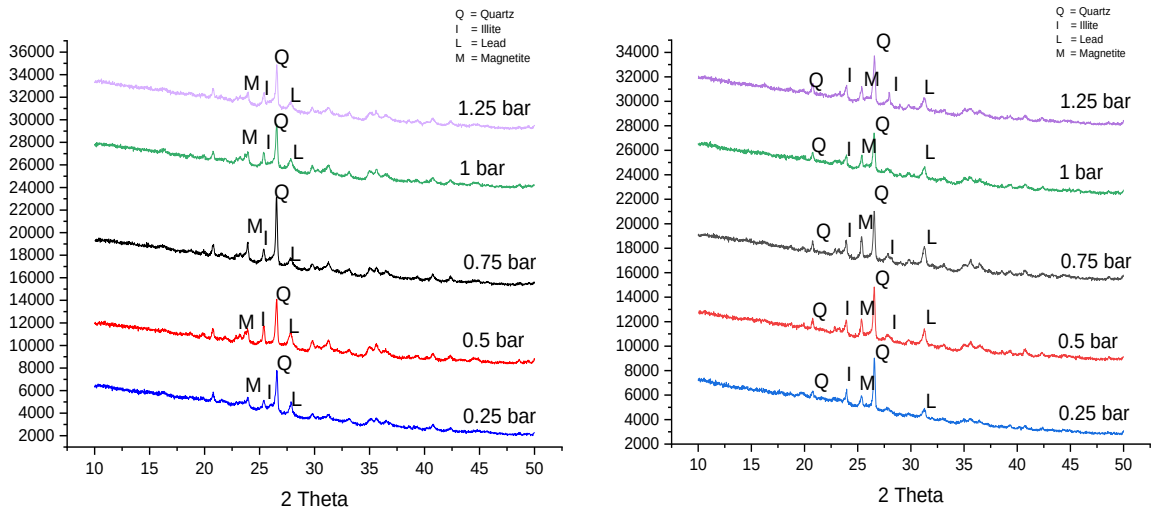

Figure 8. The XRD patterns of FAC membrane **(a)** after dead end and **(b)** crossflow filtration.

4. Conclusions

The FAC membrane with fly ash: clay composition of 65%: 35% sintered at 950° C with porosity of 40,8% and pore size of 0.9 µm, can be applied for river water treatment. The FAC ceramic membrane removed TDS, Pb, Fe, and *E. coli* from the Geudong River in North Aceh, Indonesia. Dead-end and crossflow filtering was used. The dead-end module determined that the greatest rejection of TDS, Pb, Fe, and *E. coli* was at 0.25 bar, or 70.35, 94.51, 91.43, and 98.67%. At dead-end flow, as parameter rejection drops, pressure rises. The effect of pressure on a dead-end flow system generates compaction in the circuit where the flow goes across the membrane and particles aggregate on the membrane surface. Solute concentration on the membrane surface was higher than in permeate or bait. As the pressure in a dead-end flow system increases, polarisation on the membrane surface may decrease turbidity, Pb, Fe, and *E. coli* rejection. The FAC membrane employed for crossflow filtration at 0.75 bar has the maximum lead intensity, with 96.59% rejection.

Funding

The Ministry of Research funded this research, Technology and Higher Education (KEMENRISTEK DIKTI) Republic of Indonesia, grant number 804/SP2H/AMD/LT/PNL/2020.

Acknowledgments

The Ministry of Research, Technology and Higher Education (Kemenristek Dikti) of Indonesia, the Director of Lhokseumawe State Polytechnic, and the Rector of Universitas Syiah Kuala are acknowledged.

Conflicts of Interest

The authors declare no conflict of interest.

References

1. Maharjan, A. K.; Wong, D. R. E.; Rubiyatno, R.. Level and distribution of heavy metals in Miri River, Malaysia. *Trop. Aquat. Soil Pollut.*. **2021**, *1*, 74–86, https://doi.org/10.53623/tasp.v1i2.20 .
2. El Awady, F. R.; Abbas, M. A.; Abdelghany, A. M.; El-Amir, Y. A. Silver modified hydrophytes for heavy metal removal from different water resources. *Biointerface Res. Appl. Chem.* **2021**, *11*, 14555–14563, https://doi.org/10.33263/BRIAC116.1455514563.
3. G. Mustafa; K. Wyns; S. Janssens; A. Buekenhoudt; and V. Meynen. Evaluation of the fouling resistance of methyl grafted ceramic membranes for inorganic foulants and co-effects of organic foulants. *Sep. Purif. Technol.* **2018**, 193, 29–37, https://doi.org/10.1016/j.seppur.2017.11.015.
4. Oun. A. *et al.* Tubular ultrafiltration ceramic membrane based on titania nanoparticles immobilized on macroporous clay-alumina support: Elaboration, characterization and application to dye removal. *Sep. Purif. Technol.* **2017**, *188*, 126-133, https://doi.org/10.1016/j.seppur.2017.07.005.
5. Sandhya, S. L.; Rani; Kumar, R. V. Insights on applications of low-cost ceramic membranes in wastewater treatment: A mini-review. *Case Stud. Chem. Environ. Eng.* **2021**, *4*, 100149, https://doi.org/10.1016/j.cscee.2021.100149.
6. Yin, W. X. Y.; Wang, H.; Li, D.; Jing, W.; Fan, Y. Fabrication of Mesoporous titania-Zirconia Composite Membranes Based on Nanoparticles Improved Hydrosol. *J. Colloid Interface Sci.*. **2016**, *478*, 136, https://doi.org/10.1016/j.jcis.2016.05.065.
7. S. A. Y.; Saja, S.; Bouazizi, A.; Achiou, B.; Ouaddari, H.; Karim, A.; Ouammou, M.; Aaddane, A., Bennazha, J. Fabrication of low-cost ceramic ultrafiltration membrane made from bentonite clay and its application for soluble dyes removal. *J. Eur. Ceram. Soc.* **2021**, *40*, 2453–2462, https://doi.org/10.1016/j.jeurceramsoc.2020.01.057.
8. Manni, A. *et al.* Journal of Environmental Chemical Engineering New low-cost ceramic micro fi ltration membrane made from natural magnesite for industrial wastewater treatment. *J. Environ. Chem. Eng.* **2021**, *8*, 103906, https://doi.org/10.1016/j.jece.2020.103906.
9. Abdullayev, A. G. A.; Bekheet, M.; Hanaor, D. Materials and applications for lowcost ceramic membranes," *Membranes (Basel)* **2019**, *9*, 105, https://doi.org/10.3390/membranes9090105.
10. Mouratib, R.; Achiou, B.; El Krati, M.; Younssi, S. A.; Tahiri, S. Low-cost ceramic membrane made from alumina- and silica-rich water treatment sludge and its application to wastewater filtration. *J. Eur. Ceram. Soc.* **2020**, *40*, 5942–5950, https://doi.org/10.1016/j.jeurceramsoc.2020.07.050.
11. Zou, D.; Fan, Y. State-of-the-art developments in fabricating ceramic membranes with low energy consumption. *Ceram. Int.*. **2021**, *47*, 14966–14987, https://doi.org/10.1016/j.ceramint.2021.02.195.
12. Jiang, Q.; Xie, Y.; Ji, L.; Zhong, Z.; Xing, W. Low-temperature sintering of a porous SiC ceramic filter using water glass and zirconia as sintering aids. *Ceram. Int.*. **2021**, *47*, 26125–26133, https://doi.org/10.1016/j.ceramint.2021.06.020.
13. Jiang, Q. *et al.* Lower-temperature preparation of SiC ceramic membrane using zeolite residue as sintering aid for oil-in-water separation. *J. Memb. Sci.* **2020**, *610*, 118238, https://doi.org/10.1016/j.memsci.2020.118238.
14. Fan, W.; Zou, D.; Xu, J.; Chen, X.; Qiu, M.; Fan, Y. Enhanced performance of fly ash-based supports for low-cost ceramic membranes with the addition of bauxite. *Membranes* **2021**, *11*, https://doi.org/10.3390/membranes11090711.
15. Azaman, F. *et al.* Review on natural clay ceramic membrane: Fabrication and application in water and wastewater treatment. *Malaysian J. Fundam. Appl. Sci.* **2021**, *17*, 62–78,

https://dx.doi.org/10.11113/mjfas.v17n1.2169.
16. Diana, S.; Fauzan, R.; Arahman, N.; Razi, F.; Elfiana, E. Synthesis and Characterization of Microfiltration Ceramic Membrane Based on Fly Ash and Clay Mixture Using Sintering Method. *IOP Conference Series: Materials Science and Engineering*, **2020**, https://dx.doi.org/10.1088/1757-899X/854/1/012019.
17. Oyehan, T. A.; Olabemiwo, F. A.; Tawabini, B. S.; Saleh, T. A. The capacity of mesoporous fly ash grafted with ultrathin film of polydiallyldimethyl ammonium for enhanced removal of phenol from aqueous solutions. *J. Clean. Prod.* **2020**, *263*, 121280, https://doi.org/10.1016/j.jclepro.2020.121280.
18. Das, D.; Rout P. K. Synthesis and characterization of fly ash and gbfs based geopolymer material. *Biointerface Res. Appl. Chem.* **2021**, *11*, 14506–14519, https://doi.org/10.33263/BRIAC116.1450614519.
19. Diana, S.; Fauzan, R.; Elfiana, E. Removing Escherichia Coli Bacteria in River Water using Ceramic Membrane from Mixed Clay and Fly Ash Material. *IOP Conference Series: Materials Science and Engineering* **2019**, *536*, http://dx.doi.org/10.1088/1757-899X/536/1/012089.
20. Diana, S.; Fauzan, R.; Arahman, N.; Razi, F.; Bilad M. Synthesis and Characterization of Ceramic Membrane from Fly Ash and Clay Prepared by Sintering Method at Low Temperature. *Rasayan J. Chem.* **2020**, *13*, 1335–1341, http://dx.doi.org/10.31788/RJC.2020.1335707.
21. Kamgang-Syapnjeu, P. *et al.* Elaboration of a new ceramic membrane support from Cameroonian clays, coconut husks and eggshells: Application for Escherichia coli bacteria retention. *Appl. Clay Sci.* **2020**, *198*, 105836, https://doi.org/10.1016/j.clay.2020.105836.
22. Ekpunobi, U. E.; Agbo, S. U.; and V. I. E. Ajiwe. "Evaluation of the mixtures of clay, diatomite, and sawdust for production of ceramic pot filters for water treatment interventions using locally sourced materials," *J. Environ. Chem. Eng.* **2019**, *7*, https://doi.org/10.1016/j.jece.2018.11.036.
23. Belibi Belibi, P. *et al.* Microfiltration ceramic membranes from local Cameroonian clay applicable to water treatment. *Ceram. Int.*, **2015**, *41*, 2752–2759, http://dx.doi.org/10.1016/j.ceramint.2014.10.090.
24. Khulbe, K. C.; Matsuura T. Removal of heavy metals and pollutants by membrane adsorption techniques. *Appl. Water Sci.* **2018**, *8*,.19, http://dx.doi.org/10.1007/s13201-018-0661-6.
25. Xu, Z.; Gu, S.; Rana, D.; Matsuura, T.; Lan, C. Q. Chemical precipitation enabled UF and MF filtration for lead removal. *J. Water Process Eng.* **2021**, *41*, 101987, https://doi.org/10.1016/j.jwpe.2021.101987.
26. Elma, M.; Rahma, A.; Pratiwi, A. E.; Rampun, E. L. A.. Coagulation as pretreatment for membrane-based wetland saline water desalination. *Asia-Pacific J. Chem. Eng.* **2020**, *15*, 1–7, https://doi.org/10.1002/apj.2461.
27. Elfiana, E.; Diana, S.; Fuadi, A.; Fauzan, R.. Characterization Study of Inorganic Hybrid Membrane of Mixed Activated Zeolite and Clay with PVA Adhesives using Sintering Method for colourless Peat Water. in *IOP Conference Series: Materials Science and Engineering*. **2019**, *536*, https://doi.org/10.1088/1757-899X/536/1/012036.
28. Kárászová, M.; Bourassi, M.; Gaálová, J. Membrane removal of emerging contaminants from water: Which kind of membranes should we use? *Membranes* **2020,**. *10*, 1–23, https://dx.doi.org/10.3390%2Fmembranes10110305.
29. Asif, M.; Zhang B. Z. Ceramic membrane technology for water and wastewater treatment: A critical review of performance, full-scale applications, membrane fouling and prospects. *Chem. Eng. J.* **2021**, *418*, 129481, https://doi.org/10.1016/j.cej.2021.129481.
30. He, Z.; Lyu, Z.; Gu, Q.; Zhang, L.; Wang, J. Ceramic-based membranes for water and wastewater treatment. *Colloids Surfaces A Physicochem. Eng. Asp.* **2019**, 578, 123513, https://doi.org/10.1016/j.colsurfa.2019.05.074.
31. Enten, A. C.; Leipner, M. P. I.; Bellavia, M. C.; King, L. E.; Sulchek, T. A.. Optimizing Flux Capacity of Dead-end Filtration Membranes by Controlling Flow with Pulse Width Modulated Periodic Backflush. *Sci. Rep.* **2021**, *10*, 1–11, https://www.nature.com/articles/s41598-020-57649-9.
32. Gruskevica, K.; Mezule, L. Cleaning methods for ceramic ultrafiltration membranes affected by organic fouling. *Membranes* **2021**, *11*,. 1–15, https://doi.org/10.3390/membranes11020131.
33. Di, H.; Martin, G. J. O.; Dunstan, D. E. Characterization of particle deposition during crossflow filtration as influenced by permeate flux and crossflow velocity using a microfluidic filtration system. *Front. Chem. Sci. Eng.* **2021**, *15*, 552–561, https://doi.org/10.1007/s11705-020-1962-5.
34. Zhang, L. *et al.* Hydrogenated TiO2 membrane with photocatalytically enhanced anti-fouling for ultrafiltration of surface water. *Appl. Catal. B Environ.*. **2020**, *264*, 118528, https://doi.org/10.1016/j.apcatb.2019.118528.
35. Tomczak, W. and M. Gryta. "Crossflow microfiltration of glycerol fermentation broths with citrobacter freundii," *Membranes* **2020**, *10*, https://dx.doi.org/10.3390%2Fmembranes10040067.
36. M. Krippl; A. Dürauer; and M. Duerkop. Hybrid modeling of crossflow filtration: Predicting the flux evolution and duration of ultrafiltration processes. *Sep. Purif. Technol.* **2021**, *248*, 117064, https://doi.org/10.1016/j.seppur.2020.117064.
37. WHO, Drinking Water Fact Sheet, **2021**. http://www.who.int/mediacentre/factsheets/fs391/en/ (accessed on 20 October 2021).
38. M. of H. R. of Indonesia. Clean Water Standards Ministerial Regulation No. 32/Menkes/Per/IX/2017," **2017**.
39. Hakami, M. W.; Alkhudhiri, A.; Al-Batty, S.; Zacharof, M. P.; Maddy, J.; Hilal, N. Ceramic microfiltration

membranes in wastewater treatment: Filtration behavior, fouling and prevention. *Membranes* **2020**, *10*, 1–34, https://doi.org/10.3390/membranes10090248.
40. Goswami, K. P.; Pugazhenthi, G. Credibility of polymeric and ceramic membrane filtration in the removal of bacteria and virus from water: A review. *J. Environ. Manage.* **2020**, *268*, 110583, https://doi.org/10.1016/j.jenvman.2020.110583.